INFECTION AND IMMUNITY, Aug. 1998, p. 3892–3899 Vol. 66, No. 8
0019-9567/98/$04.00+0

Infection of the Laboratory Mouse with the Intracellular Pathogen *Ehrlichia chaffeensis*

GARY M. WINSLOW,[1,2]* ERIC YAGER,[2] KONSTANTIN SHILO,[1] DORIS N. COLLINS,[1] AND FREDERICK K. CHU[1]

Wadsworth Center, New York State Department of Health, Albany, New York 12201-2002,[1] and Department of Biomedical Sciences, School of Public Health, University at Albany, Albany, New York 12201-0509[2]

Received 2 February 1998/Returned for modification 22 March 1998/Accepted 1 May 1998

To determine the basis of susceptibility and resistance to human monocytic ehrlichiosis (HME), immunocompetent and immunocompromised mice were infected with *Ehrlichia chaffeensis* and bacterial loads were measured by PCR and by immunohistochemistry. Immunocompetent (C.B-17 and C57BL/6) mice cleared the bacteria within 10 days, but immunocompromised SCID and SCID/BEIGE mice developed persistent infection in the spleen, liver, peritoneal cavity, brain, lung, and bone marrow and became moribund within 24 days. Both immunocompromised strains lack T and B lymphocytes, but the SCID/BEIGE strain is also deficient in natural killer (NK) cell function. During advanced stages of disease, the infections were associated with wasting, splenomegaly, lymphadenopathy, liver granulomas and necroses, intravascular coagulation, and granulomatous inflammation. Histochemical and immunohistochemical localization studies confirmed the presence of bacteria in tissues, and viable bacteria were cultured from infected animals. The data reveal that T and/or B cells play an essential role during resistance of immunocompetent mice to infection with *E. chaffeensis* and demonstrate the utility of immunocompromised mice as an experimental model for the study of HME.

Human monocytic ehrlichiosis (HME) is an emerging zoonotic tick-borne disease caused by infection of monocytes by the obligate intracellular monocytotropic bacterium *Ehrlichia chaffeensis* (for a review, see reference 7). In humans it is a moderate to severe acute febrile illness characterized by nonspecific symptoms such as fever, headache, malaise, and myalgia (11). HME is also associated with hematological abnormalities such as neutropenia, lymphopenia, thrombocytopenia, and anemia, as well as elevations in serum levels of liver transaminases (9, 11, 23). The pathological manifestations of HME are primarily limited to tissues associated with organs of the mononuclear phagocyte system and include bone marrow granulomas, granulomatous inflammation, focal necroses, bone marrow hyperplasia and/or hypoplasia, and megakaryocytosis (9, 24). In one study, lymphadenopathy was observed in 25% of the cases, and liver involvement was observed in 80% of all patients (11). The heaviest burden of bacteria was typically found in the liver, spleen, lymph nodes, bone marrow, and cerebrospinal fluid. Severe disease has been observed in patients with host defense abnormalities (16), and opportunistic infections have been associated with HME, suggesting that the disease may affect host immunocompetency and, in turn, susceptibility to infection by other pathogens.

Although HME has been known for over 10 years, no small-animal model has been developed for the study and experimental manipulation of the disease. Such a model system would be valuable for the identification of the host factors and cells required for resistance to infection and disease and for the rational design of therapies. In this study, immunocompetent and immunocompromised SCID (severe combined immune deficient) mice were infected with *E. chaffeensis*, and infection was monitored by PCR and immunohistochemical methods. Immunocompetent mice cleared the infection within 17 days and exhibited only minor and transient pathology. However, immunocompromised mice succumbed to infection and became moribund within 24 days. The disease in the mouse was associated with a number of characteristics that in some ways resembled those observed in humans. These included similar tropism, extensive tissue inflammation, splenomegaly, lymphadenopathy, and liver granulomas and necroses. The susceptibility of the lymphocyte-deficient immunocompromised mice supports an essential role for the adaptive immune responses during resistance to *E. chaffeensis* infection.

MATERIALS AND METHODS

Animals. C.B-17, C.B-17-*scid*, and C.B-17-*scid/bg* mice were obtained from Taconic (Tarrytown, N.Y.). C57BL/6 and C57BL/6-*scid* mice were obtained from Jackson Laboratories (Bar Harbor, Maine) or were bred in the Wadsworth Center Animal Facility under microisolater conditions in accordance with institutional guidelines for animal welfare. C.B-17 is a BALB/c congenic strain that carries the *Igh* immunoglobulin heavy-chain allotype from C57BL/6. Control (uninfected or mock-injected) mice were housed with the infected mice during the experimentation and on no occasion exhibited any signs of infection or disease. The control animals were usually analyzed at the end of the experiments.

For PCR analyses and serum collection, the animals were anesthetized, blood was collected via the retro-orbital sinus, the animals were euthanized, and the tissues were dissected and frozen on dry ice and stored at −20°C. Peritoneal exudate cells were obtained by lavage with Hanks' balanced salt solution containing 20 mM HEPES (HBSS) with the addition of 300 USP units of heparin (Sigma Chemical).

Bacteria and cell lines. The Arkansas isolate of *E. chaffeensis* (1) (kindly provided by J. Dawson, Centers for Disease Control and Prevention, Atlanta, Ga.) was used for the infections described in this study. The passage number of the isolate was not available. The bacteria were cultured in DH82 cells propagated in minimal essential medium with Earle's salts, supplemented with 1.5 g of sodium bicarbonate per liter, 2.4 mM L-glutamine, and 10% fetal bovine serum, and were maintained at 37°C in air. The bacteria were routinely passaged at a 1:10 dilution weekly to fresh DH82 cells. *E. chaffeensis* morulae in DH82 cells were detected by using a histological stain (Diff-Quik; Dade Diagnostics) after centrifugation of cells onto microscope slides in a Cytospin centrifuge (Shandon Lipshaw).

Culture of bacteria from the spleens and livers of infected mice was performed after passage of the tissues through a 100-μm nylon mesh, followed by centrifugation and washing in HBSS. Approximately 10^6 cells obtained from each tissue were used to infect DH82 cells in T-25 tissue culture flasks. The infected cells were passaged to uninfected DH82 cells at a 1:10 dilution after 5 days in culture.

* Corresponding author. Wadsworth Center, 120 New Scotland Ave., Albany, NY 12208. Phone: (518) 473-2795. Fax: (518) 486-4395/9858. E-mail: gary.winslow@wadsworth.org.

Infection of mice. Six- to 12-week-old female mice were infected intraperitoneally with *E. chaffeensis*-infected DH82 cells (typically >95% infected). There are at present no accurate methods for enumerating the number of bacteria per infected cell, but a typical DH82 cell at the peak of infection harbored on average 200 to 300 bacteria. Infected DH82 cells were isolated by scraping, washed and resuspended in HBSS, and injected into the peritoneal cavity in a volume of 0.5 ml with a 23-gauge needle. Tissues were harvested from mice and fixed for histology or were stored frozen at −20°C prior to PCR analyses. Subcutaneous injections were performed with 10^6 infected DH82 cells, in a total volume of 50 μl, at two to three sites on the back of the mouse.

Measurements of bacterial loads. Mouse tissue was digested in lysis buffer (100 mM Tris-HCl [pH 8.3], 5 mM EDTA, 0.2% sodium dodecyl sulfate, 200 mM NaCl, 0.2 mg of proteinase K per ml) at 55°C for 16 h. Fifty microliters of the digest was subjected to extraction with DNAzol (Molecular Research Center, Inc.) for 2 h at room temperature, and the released nucleic acid was precipitated in 0.6 volume of prechilled (−20°C) absolute alcohol for 2 h at room temperature. The precipitate was pelleted by centrifugation in a microcentrifuge, washed with 95% ethanol, and dissolved in 50 μl of sterile water. PCR analysis was performed in duplicate to determine the relative loads of bacteria in the tissues, as described previously (4), with the following modifications. The template amount was 0.01 A_{260} unit (0.5 μg) of total tissue DNA, and the number of cycles was reduced to 33 to ensure the linearity of the synthesis reaction. The primers were HMEIF 22-mer (5′ CAATTGCTTATAACCTTTTGGT 3′) and HME3R 24-mer (5′ CCCTATTAGGAGGGATACGACCTT 3′), located at nucleotide positions 52 to 73 and 948 to 971, respectively, in the 16S rRNA gene of *E. chaffeensis*. The PCR product was analyzed by electrophoresis on 1.5% agarose slab gels, visualized by staining with ethidium bromide, and photographed, as previously described (4). The relative amount of product was estimated from careful inspection of the product band intensity in the photograph and scored on a scale of 1 to 6, where a score of 1 indicated the smallest amount at the limit of detection and a score of 6 indicated the largest amount at saturation.

To determine the numbers of organisms in tissues, quantitative PCR was performed by comparison of tissue samples with known amounts of plasmid containing the *E. chaffeensis* 16S rRNA gene. It was determined that one U in the PCR assays (see, e.g., Fig. 1) was roughly equivalent to 200 organisms per μg of total cellular DNA from each of the tissues. The amounts of cellular DNA recovered per gram of tissue were 6.4 and 42 mg for liver and spleen, respectively, so one PCR unit corresponded to approximately 1.3×10^6 organisms per g of liver tissue and 8.3×10^6 organisms per g of spleen tissue.

Histology and immunohistochemistry. Tissue samples for histological analyses were harvested, fixed in Bouins' fixative (Polysciences, Inc.) for at least 24 h, washed repeatedly with 70% ethanol, embedded in paraffin, sectioned, and stained with hematoxylin and eosin. For immunohistochemistry, tissues were fixed in Histochoice (Amresco), embedded in paraffin, and sectioned. Sections were deparaffinized by sequential washes in Histochoice Clearing Agent (Amresco), 100% ethanol, 95% ethanol, 80% ethanol, and phosphate-buffered saline (50 mM sodium phosphate [pH 7.2], 150 mM sodium chloride). Detection of *E. chaffeensis* was performed by using biotinylated human anti-*E. chaffeensis* antiserum (a generous gift of S. Dumler, Johns Hopkins University) or biotinylated normal human serum in phosphate-buffered saline containing 5% nonfat dry milk and 1% normal human serum. Treatment with primary antibodies was followed by treatment with alkaline phosphatase-conjugated streptavidin (Sigma). The sections were developed with Fast Red TR/napthol AS-MX (Sigma Chemical) and counterstained with Mayer's hematoxylin (Sigma). Slides were mounted in aqueous mounting medium (Biomeda Corp.) and photographed with a Zeiss Axioplan microscope and Ektachrome 100 film. Images were scanned with a Polaroid Sprintscan 35 slide scanner, labeled for publication with Photoshop 3.0, and printed on a Kodak DS8650 printer.

RESULTS

Persistent infection and morbidity in immunocompromised mice. To determine the cellular basis of susceptibility and resistance to HME, immunocompromised SCID (C.B-17-*scid*) and SCID/BEIGE (SCID/BG) (C.B-17-*scid*/*bg*) mice were infected with *E. chaffeensis* (Arkansas isolate) (1). SCID mice are deficient in the production of T and B cells but exhibit normal function of myeloid cells, antigen-presenting cells, and natural killer (NK) cells (6, 19). SCID/BG mice carry in addition the *beige (bg)* mutation. The effects of the *bg* mutation are pleiotropic and result in impaired neutrophil chemotaxis and bactericidal activity, impaired NK cell functions, defects in cytotoxic T-cell responses, and impaired macrophage-mediated antimicrobial activity (19, 22). Because *E. chaffeensis* is an obligate intracellular pathogen, the mice were inoculated with infected canine histiocyte cells (DH82; 2.5×10^6 to 5.0×10^6 per infection) by intraperitoneal injection. At various times after infection, tissues were isolated and assays for bacteria were performed. There are at present no established methods for enumeration of *E. chaffeensis*, so bacterial loads were estimated by PCR assay for *E. chaffeensis* 16S ribosomal DNA (5).

Bacteria were detected in most tissues examined in the immunocompetent mice within 3 days after infection, but these mice cleared the bacteria within 17 days (Fig. 1). In contrast, widespread and persistent infection occurred in the immunocompromised SCID and SCID/BG mice (Fig. 1a). By day 17 postinfection bacteria were found in the liver, spleen, lymph nodes, peritoneal exudate cells, lung, brain, bone marrow, and peripheral blood. Detection of the bacteria in these tissues was not due to blood contamination, because significant numbers of bacteria were usually not detected in the blood until later times after infection. Bacteria were also not detected after the injection of heat-killed infected DH82 cells (data not shown). On day 24 postinfection the immunocompromised animals had become moribund and were euthanized. Similar results were obtained with immunocompetent (C57BL/6) and immunocompromised (C57BL/6-*scid*) mice (Fig. 1b), indicating that the susceptibility of the SCID mice was not significantly influenced by genetic background of the hosts. Thus, T cells and B cells, which are absent in both the SCID and SCID/BG strains, play a critical role in immunity to infection by *E. chaffeensis* in the mouse. C57BL/6-*bg*/*bg* mice were not susceptible to infection, which indicated that this mutation alone was not critical for host susceptibility.

It is unlikely that the bacteria identified in the tissues were due to persistence of the infected DH82 cells in the immunocompromised mice, because the infected DH82 cells were found to be lysed within a few days when left in culture (not shown). Furthermore, transfer of infected splenocytes obtained from C.B-17-*scid*/*bg* mice at 17 days postinfection into C.B-17-*scid*/*bg* mice also resulted in persistent infection (Fig. 1c).

Culture of *E. chaffeensis* isolated from infected mice. The presence of the bacteria in the mice revealed by the PCR analyses was confirmed by histochemical staining of peritoneal exudate cells and liver cells from infected animals (Fig. 2). Typical *E. chaffeensis* morulae were readily detected in peritoneal macrophages in SCID mice (Fig. 2a), and the number of infected peritoneal macrophages in the immunocompromised mice increased with time. Intracellular bacteria were also detected in smears of liver tissue from SCID mice at 17 days postinfection (Fig. 2b). To confirm that the bacteria detected in the infected mice were viable, infected cells were isolated from spleen and liver tissue from mice that had been infected 10 days earlier and were used to infect DH82 cells. Within 7 days bacteria were readily identified in the DH82 cultures, and the bacteria proliferated after passage in DH82 cells (Fig. 2c). Thus, the bacteria cultured from the mouse cells were viable and fully capable of infection of DH82 cells.

Weight loss and splenomegaly in infected mice. Infection in the immunocompromised mice was associated with wasting, as evidenced by up to a 25% loss of body weight by day 17 postinfection (Fig. 3a). In addition, all of the infected mice exhibited pronounced splenomegaly (Fig. 3b). In the immunocompetent C.B-17 mice, which recovered from infection, spleen weight was increased by about 30% at 10 days postinfection and recovered to normal levels within 24 days. Splenomegaly in the immunocompromised C.B-17-*scid* and C.B-17-*scid*/*bg* mice was also evident by day 10 postinfection, but spleen weight continued to increase until the time of euthanization. Splenomegaly was most pronounced in the SCID/BG mice, in which spleen weight increased as much as 20-fold during the course of the infection (Fig. 3b).

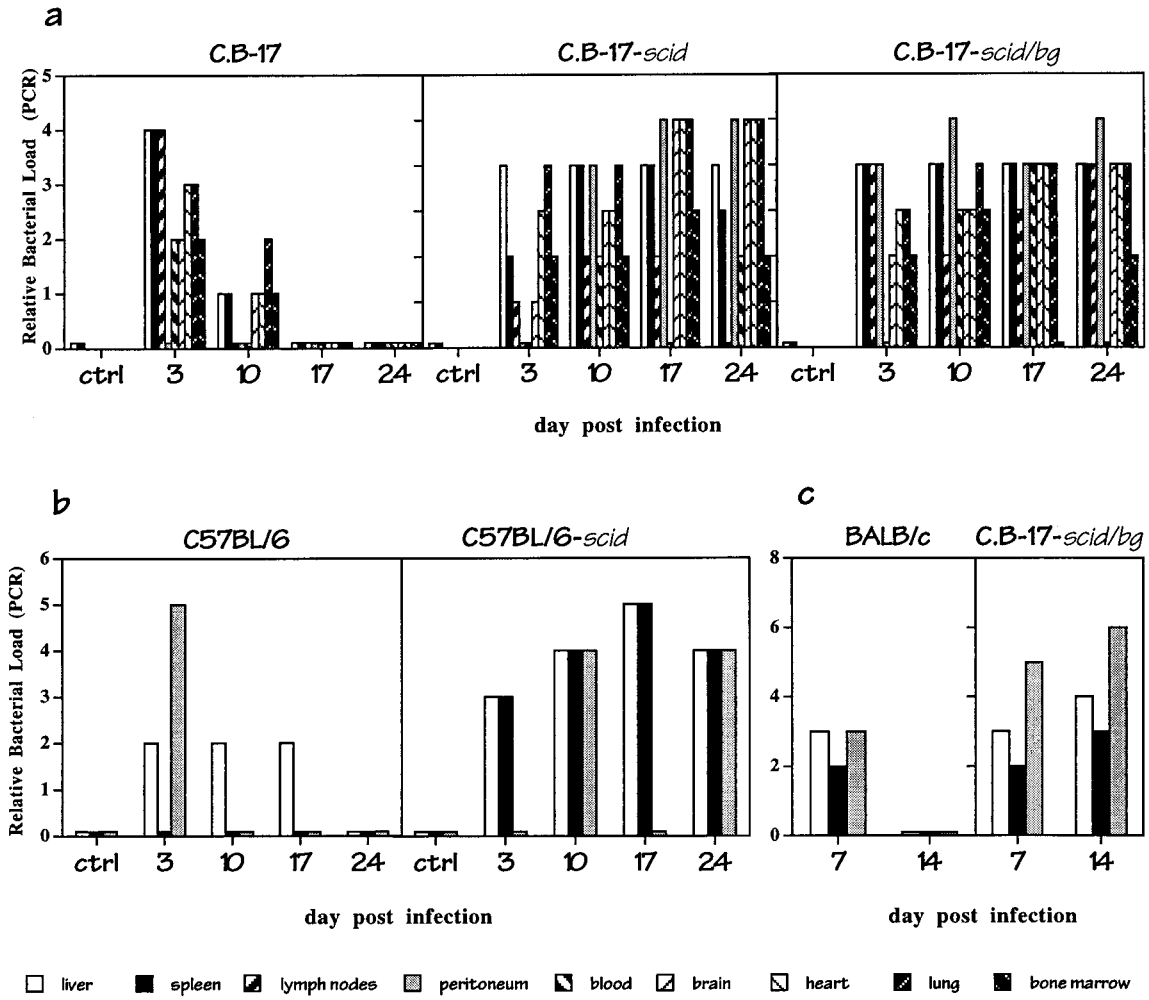

FIG. 1. Persistent infection by *E. chaffeensis* in immunocompromised, but not immunocompetent, mice. Mice were inoculated intraperitoneally with 2.5×10^6 to 5.0×10^6 *E. chaffeensis*-infected DH82 cells (>95% infected) or with HBSS (ctrl). The mice were sacrificed on the indicated day postinfection, and the bacterial loads in the indicated tissues were determined by semiquantitative PCR for *E. chaffeensis* 16S ribosomal DNA. The histograms indicate the relative levels of bacteria in the tissues (a score of 1 to 6, where 1 and 6 indicate products at the limit of detection and at saturation, respectively). The assays were performed with equivalent amounts of total cellular DNA. Each PCR unit corresponded to approximately 200 organisms per microgram of total cellular DNA (for details, see Materials and Methods), but due to the possible loss of linearity in the PCR assays, bacterial loads may be underestimated at high levels of bacterial infection. One mouse of each strain was analyzed on each of the indicated days. (a) Infection of C.B-17, C.B-17-*scid*, and C.B-17-*scid/bg* mice. (b) Infection of C57BL/6 and C57BL/6-*scid* mice. (c) BALB/c (C.B-17 *Igh* congenic) and C.B-17-*scid/bg* mice were infected intraperitoneally with 10^7 splenocytes obtained from a C.B-17-*scid/bg* mouse at 17 days postinfection, and bacterial loads were measured 7 and 14 days later. The experiments have been repeated at least three times with similar results. In all experiments the control mice were housed in the same cages as the infected mice.

Dose response and effect of route of inoculation. To determine the dose of infected DH82 cells required to cause persistent infection and disease, graded doses of infected DH82 cells (10^2 to 10^6) were administered to SCID and SCID/BG mice, and bacterial loads and spleen weights were monitored over time. It is not yet possible to precisely quantitate the number of *E. chaffeensis* organisms in an infected cell, but it was estimated by histological methods that the infected DH82 cells used in this experiment contained 200 to 300 organisms per cell.

PCR analysis of liver tissue from infected mice indicated that all of the immunocompromised mice became persistently infected, irrespective of the initial dose (Fig. 4a). All of the SCID/BG mice, and all of the SCID mice except those that received the lowest inoculum (250 infected cells), became moribund within 24 days. Splenomegaly was present in the infected SCID/BG mice irrespective of dose but varied among the SCID mice at these doses (Fig. 4b). Thus, the immunocompromised mice were susceptible to infection with as few as 250 infected DH82 cells, although splenomegaly appeared to be more limited in the SCID mice.

To examine the effect of the route of administration, immunocompromised SCID mice were also infected via subcutaneous injection (Fig. 4c). The SCID mice became persistently infected, although bacteria were not detected in the liver and spleen until day 10. Thus, bacterial dissemination appeared to be delayed relative to that in animals infected via intraperitoneal injection (Fig. 1).

Pathology in the infected mice. The persistent infection of the SCID/BG mice was associated with demonstrable pathology. In addition to the splenomegaly described above, most notable was the presence of areas of liver necrosis, beginning as early as day 10 postinfection. Grossly, the liver surface exhibited numerous pale areas of necrosis (Fig. 5a). The his-

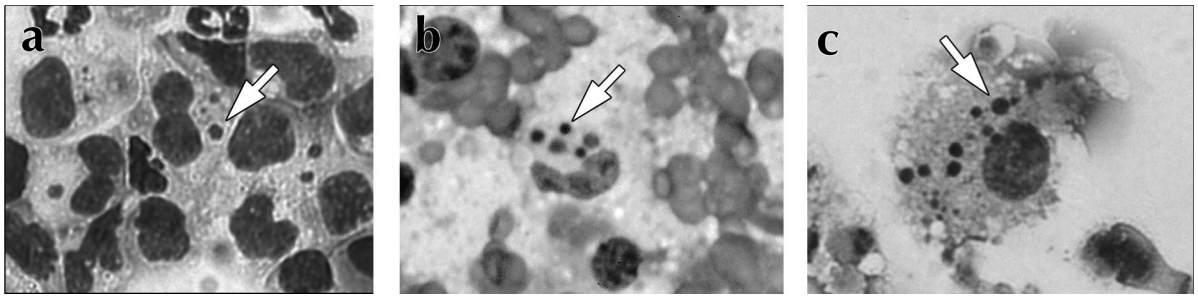

FIG. 2. Identification of *E. chaffeensis* in infected mice and after in vitro culture. To detect *E. chaffeensis*, cells from infected mice were stained with the histochemical stain Diff-Quik. Arrows indicate characteristic *E. chaffeensis* morulae. (a) Identification of *E. chaffeensis* in peritoneal macrophages obtained by lavage from C.B-17-*scid* mice on day 17 postinfection. (b) Morulae in cells obtained from a C.B-17-*scid* liver on day 17 postinfection. (c) Detection of *E. chaffeensis* in DH82 cells following incubation with infected C.B-17-*scid/bg* liver cells harvested 10 days postinfection. The bacteria were successfully passaged two times in DH82 cells.

topathology of the liver exhibited a variety of lesions. Most striking were the numerous areas of acidophilic hepatocyte necrosis with peripheral inflammatory reaction and thrombotic vascular occlusion, many in portal vessels (Fig. 5b and c). Vascular lesions varied from early stages of intravascular coagulation to partial thrombosis and complete organization. Early areas of necrosis were noted as apoptosis of individual hepatocytes. Other lesions were numerous granulomas, some varying from small collections of leukocytic foci to larger aggregates of mononuclear macrophages admixed with polymorphonuclear leukocytes. Granulomas were present in portal areas and appeared to associate with and compress portal vessels (Fig. 5).

The SCID/BG spleens, which lack characteristic lymphoid follicles due to the absence of T and B lymphocytes (6), were characterized only by general leukocyte metaplasia. Marked lymphadenopathy was observed in the SCID/BG mice, and infection in the heart was associated with pericarditis; abdominal hemorrhaging was often noted in the SCID/BG mice, and bone marrow hypercellularity was noted in both strains of immunocompromised mice. Granulomatous infiltration was also detected in the meninges of the brain (not shown).

Pathology in the SCID mice generally mirrored that seen in the SCID/BG mice except that it was in general less severe. Although massive leukocytic infiltration was observed in the livers of infected SCID mice, coagulative necroses were not as common and their appearance was often delayed relative to that in the SCID/BG mice.

In immunocompetent C.B-17 mice, granulomatous infiltration was evident in the liver within 3 days postinfection (Fig. 5d). The infiltrates appeared to be composed of polymorphonuclear cells and macrophages, as well as lymphocytes. Apoptotic hepatocytes were also observed and were found to be associated with areas of inflammation. Infiltration was readily observed on day 3 postinfection but was diminished at later periods after infection. No other tissue lesions were detected in the immunocompetent mice.

Immunolocalization of *E. chaffeensis* in tissues of infected mice. Human anti-*E. chaffeensis* sera were used to detect *E. chaffeensis* in fixed paraffin sections of infected tissues (Fig. 6).

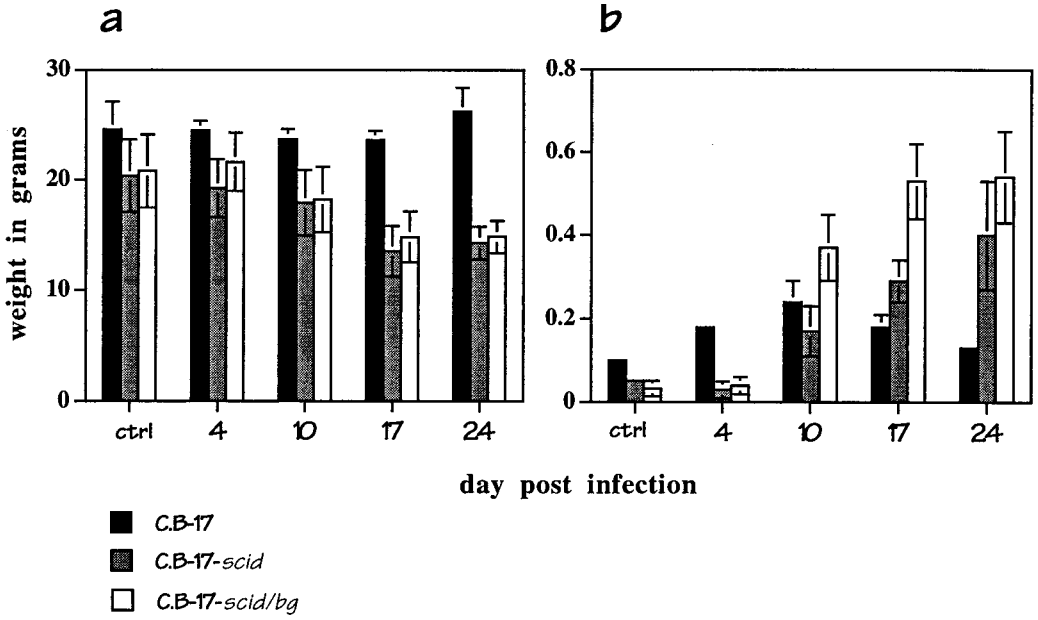

FIG. 3. Wasting and splenomegaly in infected mice. C.B-17, C.B-17-*scid* and C.B-17-*scid/bg* mice were not infected (ctrl) or were infected with 2.5×10^6 infected DH82 cells. Body (a) and spleen (b) weights were determined on the indicated days postinfection. The data shown are the means and standard deviations of the values obtained on each day from three mice of each strain.

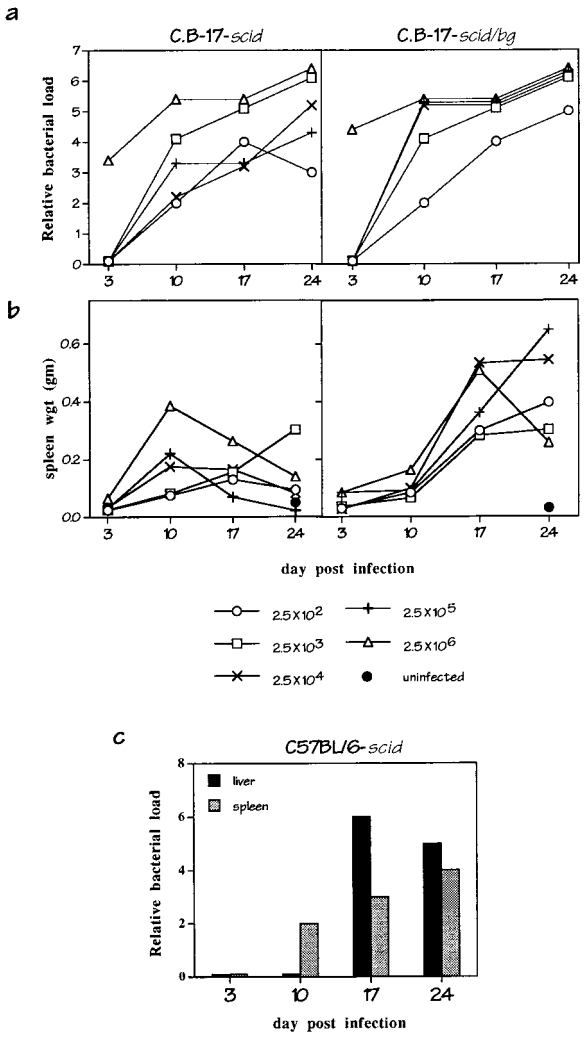

FIG. 4. Dose response and effect of inoculation route. C.B-17-*scid* and C.B-17-*scid*/*bg* were infected with graded numbers of infected DH82 cells (>95% infected) as indicated, and PCR analyses of bacteria loads in liver tissue (a) or measurements of spleen weights (b) were performed. (c) Effect of inoculation route. C57BL/6-*scid* mice were inoculated subcutaneously with 10^6 infected DH82 cells, and analyses of bacteria were performed by PCR.

Infected cells were identified in the livers of SCID/BG mice as early as 10 days after infection, and the number of infected cells increased throughout the postinfection period (Table 1). Bacteria were detected in the sinusoidal cells in the liver, which were presumably Kupffer cells. The infected cells were not found to be localized to areas of inflammation in the liver but appeared to be randomly distributed throughout sinusoidal space (Fig. 6a). The number of morulae detected in the liver differed from that typically observed in DH82 cells in that the infected cells in the liver often contained only one or a few very large morulae (Fig. 6).

E. chaffeensis-infected cells were also detected in the spleens of the immunocompromised mice (Fig. 6b). As in the liver, infected splenocytes were first observed at 10 days postinfection, and their numbers increased during the following 2 weeks. *E. chaffeensis*-infected cells were also detected in low numbers (one to a few infected cells per field) in several other tissues examined in the SCID and SCID/BG mice, including lung, heart, brain, and kidney (data not shown). In these tissues the bacteria were detected within areas of granulocytic infiltration. Bacteria have not yet been detected in tissues of infected immunocompetent mice (C.B-17 or C57BL/6), even though these tissues were positive by PCR assays, indicating that immunohistochemical methods may fail to detect low levels of bacterial infection.

DISCUSSION

The data presented in this study demonstrate that immunocompromised mice can be persistently and fatally infected with *E. chaffeensis*. This is the first report of an experimental animal model for HME. The bacteria were detected in the infected mice by using PCR, histochemistry, and immunohistochemistry. The bacteria were viable, because they could be cultured in vitro from infected tissues. Moreover, infection and disease could result after infection of C.B-17-*scid*/*bg* mice with as few as 250 infected DH82 cells, indicating that the bacteria were able to multiply in the immunocompromised hosts. Persistent infection of the immunocompromised mice was not dependent on the characteristics of the infected host cell, because infected mouse splenocytes could also transfer disease, nor was it dependent on the route of needle inoculation. It is not yet known if or how tick inoculation might influence the immune response in the mouse, although no differences between needle and tick inoculation were reported after infection of the mouse with the agent of human granulocytic ehrlichiosis (20).

The PCR assays used to measure bacterial colonization were only semiquantitative, so it was possible to obtain only estimates of bacterial numbers during infection. Moreover, the PCR assays probably provided an underestimation of high bacterial loads, so the real kinetics of bacterial infection were not revealed by the PCR data. Rather, it is likely that the bacteria proliferated throughout the postinfection period in the immunocompromised mice, as was suggested by the immunohistochemistry analyses shown in Table 1.

Critical role of the adaptive immune response. Immunocompetent C.B-17 and C57BL/6 mice typically developed infection within 3 days of administration of bacteria, but bacteria were not detected by PCR assay beyond 17 days, and the animals exhibited only transient liver inflammation. Previous studies of infected C3H/HeJ mice detected bacteria as late as 28 days postinfection by nested PCR (21), but the C3H/HeJ mice were not observed to develop any pathology. The prolonged persistence of the bacteria in the C3H/HeJ mice may have been due to the use of a different mouse strain or to the greater sensitivity of the nested PCR technique used in the previously published studies. The relevance of the observation of only transient infection in the immunocompetent laboratory mice to the suitability of the mouse as a natural reservoir for *E. chaffeensis* in the wild is unknown.

In contrast to the immunocompetent mice, both SCID and SCID/BG mice were unable to clear the infection, which became established in all tissues that were examined by PCR. Therefore, adaptive immunity, mediated by T and B lymphocytes, is critical for elimination of *E. chaffeensis*. Although all immunocompromised mice developed disease, splenomegaly and liver necrosis were typically found to be more pronounced in the SCID/BG mice. This suggested that the deficient NK cell function in the SCID/BG mice also contributed to disease severity. Homozygous C57BL/6-*bg* mice were not susceptible to disease, however, so NK cell activity was not by itself essential for disease resistance in mice of the C57BL/6 background and presumably other genetic backgrounds.

The involvement of T cells was not unexpected, because both $\alpha\beta$ and $\gamma\delta$ T-cell responses are characteristically gener-

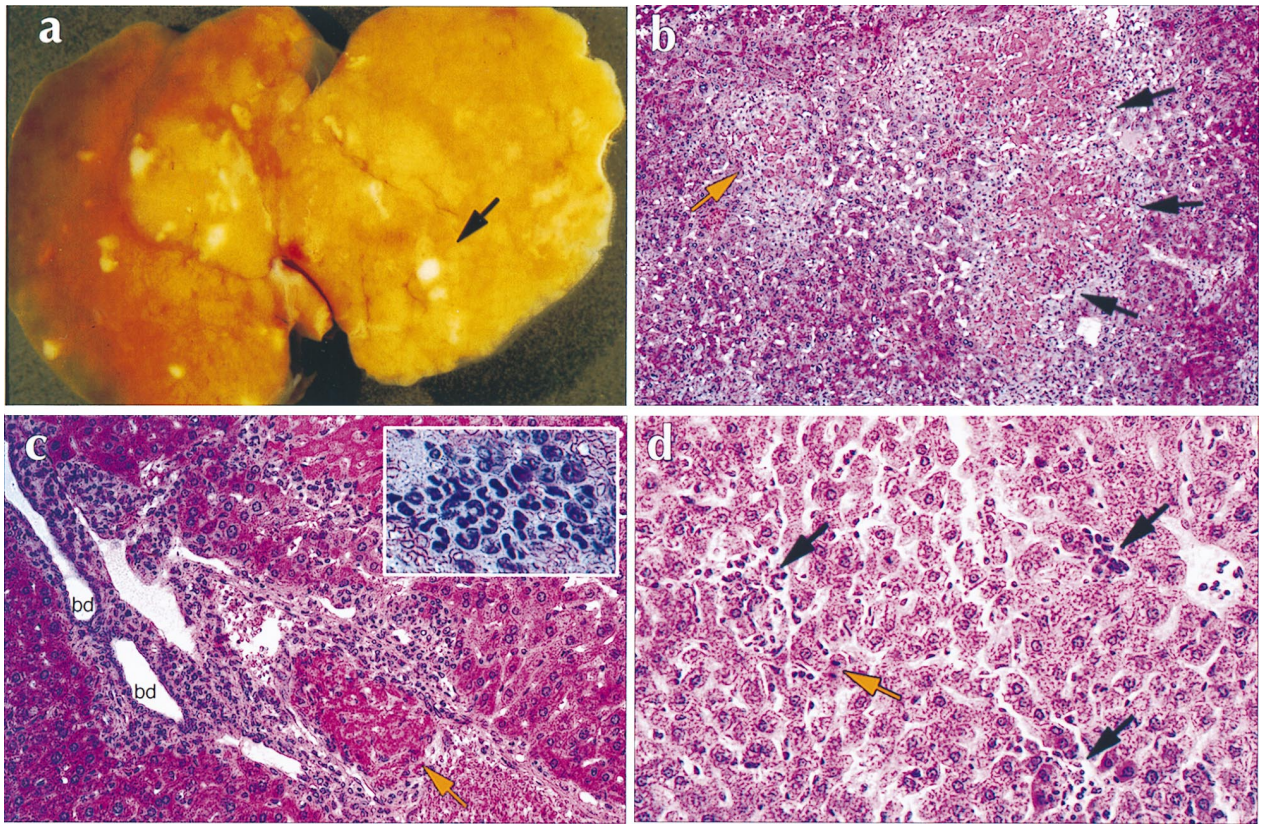

FIG. 5. Histopathology of *E. chaffeensis* infection in C.B-17-*scid/bg* and C.B-17 mice. (a) Whole mount of a liver of a C.B-17-*scid/bg* mouse at 17 days postinfection. The arrow indicates an area of necrosis. (b to d) Hematoxylin-eosin staining of paraffin sections of infected livers. (b) C.B-17-*scid/bg* liver showing extensive areas of acidophilic coagulative necrosis of entire lobule (orange arrow) and confluent lobules (black arrows). Note the inflammatory infiltrate at the periphery of necrotic lobules. Magnification, ×100. (c) C.B-17-*scid/bg* liver showing portal tract with organizing thrombus in portal vein (orange arrow). There is a diffuse mononuclear inflammatory infiltrate in the portal tract penetrating the limiting plate and bordering hepatocytes. bd, bile ducts. Magnification, ×250. The inset shows a high-magnification view of a typical granulomatous infiltrate in a C.B-17-*scid/bg* liver. (d) Presence of lymphohistiocytic infiltrates in the liver of a C.B-17 mouse at 3 days postinfection (black arrows). Note apoptotic hepatocytes, characterized by condensed nuclei (orange arrow). Magnification, ×250.

ated against intracellular bacteria (12, 15). Because the monocyte is the target of infection in humans and mice, the role of the T and/or B cells may be to directly or indirectly activate macrophage microbiocidal activities. Resistance to mycobacteria and *Listeria* is dependent in part on antigen-specific CD4 or CD8 T cells, or NK cells, for the production of gamma interferon and subsequent activation of macrophage bacteriocidal functions (2, 14). Similarly, during ehrlichia infection, T cells may produce inflammatory cytokines which provide macrophages with appropriate signals to induce bacterial clearance. Gamma interferon has been shown to prime human monocytes to kill *E. chaffeensis* in vitro (3). However, passive transfer of

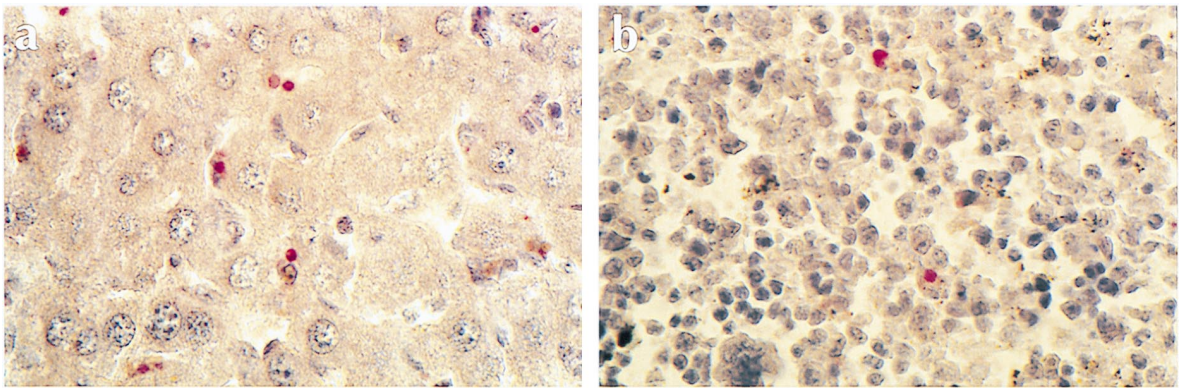

FIG. 6. Immunohistochemical localization of *E. chaffeensis*. Paraffin sections of liver (a) and spleen (b) tissues from C.B-17-*scid/bg* mice (day 17 postinfection) were stained with biotinylated human anti-*E. chaffeensis* serum followed by alkaline phosphatase-conjugated streptavidin, developed with Fast Red TR/napthol AS-MX, and counterstained with hematoxylin (seen as brown to blue staining). The intense red coloration indicates the presence of *E. chaffeensis* morulae. No staining was observed with biotinylated normal human serum and secondary antibodies, and very similar results were obtained with C.B-17-*scid* mice. Magnification, ×400.

TABLE 1. Multiplication of *E. chaffeensis* in infected tissues of immunocompromised mice

Day postinfection	No. of infected cells per field[a] in:			
	Liver[b]		Spleen	
	C.B-17-*scid* mice	C.B-17-*scid*/*bg* mice	C.B-17-*scid* mice	C.B-17-*scid*/*bg* mice
3	0	0	ND[c]	ND
10	1 ± 1	0.8 ± 0.83	ND	ND
17	3.2 ± 2.4	4.6 ± 1.7	7.0 ± 1.3	4.9 ± 3.1
24	11.7 ± 4.3	2.1 ± 2.1[d]	7.3 ± 1.1	8.5 ± 4.2

[a] Values are the means and standard deviations of *E. chaffeensis*-positive cells detected in the tissues of the indicated strains by immunohistochemistry (5 to 10 fields per group; magnification, ×1,000).

[b] Liver sections contained on average 90.5 ± 16.4 hepatocytes/field; spleen sections contained 482 ± 120 cells/field.

[c] ND, not determined.

[d] Substantial necrosis was present in these tissue sections.

antibodies protected mice from ehrlichia infection induced both by *Ehrlichia risticci* and by the agent of human granulocytic ehrlichiosis (13, 20), so a role for humoral responses in protection from *E. chaffeensis* infection should also be considered.

Comparison of ehrlichiosis in mice and humans. *E. chaffeensis* infection in the immunocompromised mice resulted in severe and fatal disease. The infected immunocompromised mice exhibited marked splenomegaly, lymphadenopathy, intravascular thromboses, abdominal hemorrhaging, extensive granulomatous infiltration, and focal liver necroses. HME patients exhibit a spectrum of clinical and laboratory abnormalities that vary among individuals (24). The genetic variability in infected immunocompetent and immunodeficient humans makes direct comparisons of the disease in humans and mice problematic. Moreover, the number of case studies of HME has been limited, so a complete characterization of the disease in humans has not been possible. However, some of the characteristics and pathological manifestations observed in the immunocompromised mice are similar to those in HME.

E. chaffeensis is monocytotropic in humans, and all available evidence suggests that this is also true in mice. Histological staining of mouse peritoneal exudate cells demonstrated that the bacteria were present in macrophages but not in granulocytes. In situ localization of the bacteria in mouse liver suggested that the hepatic sinusoidal cells, presumably Kupffer cells, were infected, as in humans (10). Lymphadenopathy and abdominal hemorrhaging have been observed during HME (10, 11), and the latter may relate to the disseminated intravascular coagulation, thromboses, and hemorrhaging observed in the mouse. HME is also associated with a number of hematological abnormalities, including leukopenia and thrombocytopenia (9), but it has not yet been determined if these abnormalities also occur in the mouse.

Lymphohistiocytic infiltration, focal liver necroses, and granulomatous lesions have been reported for HME (8, 24) and may be comparable to some of the pathology observed in the mouse. However, there is no evidence in humans for the massive liver destruction observed during later stages of infection in the SCID/BG and, to a lesser extent, in the SCID mice. Ehrlichiosis in the immunocompromised mice may therefore represent a form of the disease that is not typically seen in immunocompetent humans. Perhaps the transient inflammation observed in the immunocompetent mice more closely resembles the features of the disease experienced by most immunocompetent humans. Differences between ehrlichiosis in mice and that in humans clearly exist, but the basic immune mechanisms that operate during resistance to *E. chaffeensis* infection in humans and mice are almost certainly the same.

The cause of death in the immunocompromised mice is currently unknown. Although liver destruction was extensive in the immunocompromised mice, it is not known if this was sufficient to cause the animals to die. The disease in the mouse appeared to be similar to that induced by inflammatory cytokines (e.g., wasting and inflammation) and suggested that the disease in the immunocompromised mice was associated with disregulation of inflammatory cytokines such as tumor necrosis factor alpha, perhaps associated with sepsis (17).

Susceptibility and resistance in humans. It is not known why some humans appear to be susceptible to HME. Most exposed humans remain asymptomatic or do not seek medical attention (18). It appears that immunocompromised individuals are highly susceptible to HME (16), but it is not clear why other patients who are not obviously immunocompromised on occasion become seriously infected and ill. Although many other factors besides host immunocompetence are likely to influence disease susceptibility (e.g., bacterial strain, dose, host age, and coinfection with other pathogens), it is possible that more subtle differences in the immune status of the host play an important role in host resistance. Such differences in host immunity might include variations in cytokine responses, T-cell activation, macrophage activities, and others. These differences can be readily addressed and manipulated experimentally by using the mouse infection model described here. Information gained from these studies will facilitate development of treatment regimens and therapy, including the rational design of vaccines.

ACKNOWLEDGMENTS

We thank S. Wong, J. Dawson, and S. Dumler for advice and critical reagents and D. Murphy and K. McDonough for critical reading of the manuscript. We also appreciate the assistance of the Wadsworth Immunology Core facilities and the Laboratory of Anatomical Pathology. We also thank D. Mix, M. Reilly, H. Ling, D. Decker, and M. Tackley for excellent technical assistance and A. Bernat and the Wadsworth Center Photography and Illustration Unit for assistance with the graphics.

This work is supported in part by Public Health Service grant CA69710-02.

REFERENCES

1. **Anderson, B. E., J. E. Dawson, D. C. Jones, and K. H. Wilson.** 1991. *Ehrlichia chaffeensis*, a new species associated with human ehrlichiosis. J. Clin. Microbiol. **29:**2838–2842.
2. **Bancroft, G. J., and J. P. Kelly.** 1994. Macrophage activation and innate resistance to infection in SCID mice. Immunobiology **191:**424–431.
3. **Barnewall, R. E., and Y. Rikihisa.** 1994. Abrogation of gamma interferon-induced inhibition of *Ehrlichia chaffeensis* infection in human monocytes with iron transferrin. Infect. Immun. **62:**4808–4810.
4. **Chu, F. K.** Rapid and sensitive PCR-based detection and differentiation of etiologic agents of human granulocytic and monocytotropic ehrlichioses. Mol. Cell. Probes, in press.
5. **Chu, F. K., G. M. Winslow, R. Duncan, J. S. Dumler, D. Perlman, and S. Wong.** 1998. Unpublished data.
6. **Custer, R. P., G. C. Bosma, and M. J. Bosma.** 1985. Severe combined immunodeficiency (SCID) in the mouse. Am. J. Pathol. **120:**464–477.
7. **Dumler, J. S., and J. S. Bakken.** 1995. Ehrlichial diseases of humans: emerging tick-borne infections. Clin. Infect. Dis. **20:**1102–1110.
8. **Dumler, J. S., P. Brouqui, J. Aronson, J. P. Taylor, and D. H. Walker.** 1993. Identification of ehrlichia in human tissue. N. Engl. J. Med. **325:**1109–1110.
9. **Dumler, J. S., J. E. Dawson, and D. H. Walker.** 1993. Human ehrlichiosis: hematopathology and immunohistologic detection of *Ehrlichia chaffeensis*. Hum. Pathol. **24:**391–396.
10. **Dumler, J. S., W. L. Sutker, and D. H. Walker.** 1993. Persistent infection with *Ehrlichia chaffeensis*. Clin. Infect. Dis. **17:**903–905.
11. **Fishbein, D. B., J. E. Dawson, and L. E. Robinson.** 1994. Human ehrlichiosis in the United States, 1985 to 1990. Ann. Intern. Med. **120:**736–743.
12. **Kaufmann, S. H. E.** 1993. Immunity to intracellular bacteria. Adv. Immunol. **11:**129–163.

13. **Kaylor, P. S., T. B. Crawford, T. F. McElwain, and G. H. Palmer.** 1991. Passive transfer of antibody to *Ehrlichia risticii* protects mice from ehrlichiosis. Infect. Immun. **59:**2058–2062.
14. **Magee, D. M., and E. J. Wing.** 1988. Cloned L3T4$^+$ T lymphocytes protect mice against *Listeria monocytogenes* by secreting IFN-γ. J. Immunol. **141:** 3203–3207.
15. **Modlin, R. L., C. Pirmez, F. M. Hofman, V. Torigian, K. Uyemura, T. H. Rea, B. R. Bloom, and M. B. Brenner.** 1989. Lymphocytes bearing antigen-specific γδ T-cell receptors accumulate in human infectious disease lesions. Nature **339:**544–549.
16. **Paddock, C. D., D. P. Suchard, K. L. Grumbach, W. K. Hadley, R. L. Kerschmann, N. W. Abbey, J. E. Dawson, B. E. Anderson, K. G. Sims, J. S. Dumler, and B. G. Herndier.** 1993. Fatal seronegative ehrlichiosis in a patient with HIV infection. N. Engl. J. Med. **329:**1164–1167.
17. **Pajkrt, D., and S. J. H. van Deventer.** 1996. The cellular response in sepsis. Curr. Top. Microbiol. Immunol. **216:**119–131.
18. **Peterson, L. R., L. A. Sawyer, D. B. Fishbein, P. W. Kelley, R. J. Thomas, L. A. Magnarelli, M. Redus, and J. E. Dawson.** 1989. An outbreak of ehrlichiosis in members of an army reserve unit exposed to ticks. J. Infect. Dis. **159:**562–568.
19. **Shultz, L. D., and C. L. Sidman.** 1987. Genetically determined murine models of immunodeficiency. Annu. Rev. Immunol. **5:**367–403.
20. **Sun, W., J. W. IJdo, S. R. Telford III, E. Hodzic, Y. Zhang, S. W. Barthold, and E. Fikrig.** 1997. Immunization against the agent of human granulocytic ehrlichiosis in a murine model. J. Clin. Invest. **100:**3014–3018.
21. **Telford, S., R., III, and J. E. Dawson.** 1996. Persistent infection of C3H/HeJ mice by *Ehrlichia chaffeensis*. Vet. Microbiol. **52:**103–112.
22. **Vasquez-Torres, A., J. Jones-Carson, and E. Balish.** 1994. Candidacidal activity of macrophages from immunocompetent and congenitally immunodeficient mice. J. Infect. Dis. **170:**180–188.
23. **Walker, D. H., and J. S. Dumler.** 1996. Emergence of ehrlichioses as human health problems. Emerg. Infect. Dis. **2:**18–29.
24. **Walker, D. H., and J. S. Dumler.** 1997. Human monocytic and granulocytic ehrlichioses. Arch. Pathol. Lab. Med. **121:**785–791.

Editor: T. R. Kozel